Chapter Twelve
Robust Performance

However, by building an amplifier whose gain is deliberately made, say 40 decibels higher than necessary (10000 fold excess on energy basis), and then feeding the output back on the input in such a way as to throw away that excess gain, it has been found possible to effect extraordinary improvement in constancy of amplification and freedom from non-linearity.

Harold S. Black, "Stabilized Feedback Amplifiers", 1934 [Bla34].

This chapter focuses on the analysis of robustness of feedback systems, a large topic for which we provide only an introduction to some of the key concepts. We consider the stability and performance of systems whose process dynamics are uncertain and derive fundamental limits for robust stability and performance. To do this we develop ways to describe uncertainty, both in the form of parameter variations and in the form of neglected dynamics. We also briefly mention some methods for designing controllers to achieve robust performance.

12.1 MODELING UNCERTAINTY

Harold Black's quote above illustrates that one the key uses of feedback is to provide robustness to uncertainty ("consistency of amplification"). It is one of the most useful properties of feedback and is what makes it possible to design feedback systems based on strongly simplified models.

One form of uncertainty in dynamical systems is that the parameters describing the system are unknown, or *parametric uncertainty*. A typical example is the variation of the mass of a car, which changes with the number of passengers and the weight of the baggage. When linearizing a nonlinear system, the parameters of the linearized model also depend on the operating condition. It is straightforward to investigate effects of parametric uncertainty simply by evaluating the performance criteria for a range of parameters. Such a calculation will directly reveal the consequences of parameter variations. We illustrate by a simple example.

Example 12.1 Cruise control
The cruise control problem was described in Section 3.1 and a PI controller was designed in Example 10.3. To investigate the effect of parameter variations we will choose a controller designed for a nominal operating condition corresponding to mass $m = 1600$, fourth gear ($\alpha = 12$) and speed $v_e = 25$ m/s; the controller gains are $k = 0.72$ and $k_i = 0.18$. Figure 12.1a shows the velocity v and the throttle u when encountering a hill with a 3° slope with masses in the range $1600 < m < 2000$, gear ratios 3 to 5 ($\alpha = 10$, 12 and 16) and velocity $10 \leq v \leq 40$

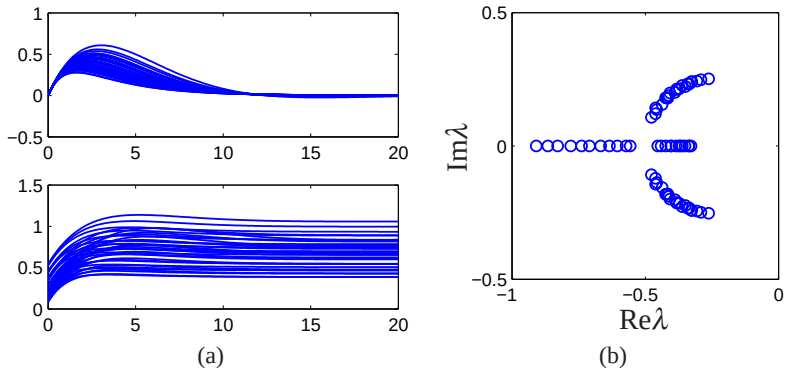

Figure 12.1: Responses of the cruise control system to a slope increase of 3° (left) and the eigenvalues of the closed loop system (right). Model parameters are swept over a wide range.

m/s. The simulations were done using models that were linearized around the different operating conditions. The figure shows that there are variations in the response but that they are quite reasonable. The largest velocity error is in the range of 0.2 to 0.6 m/s, and the settling time is about 15 s. The control signal is marginally larger than 1 in some cases which implies that the throttle is fully open. A full nonlinear simulation using a controller with windup protection is required if we want to explore these cases in more detail. Figure 12.1b shows the eigenvalues of the closed loop system for the different operating conditions. The figure shows that the closed loop system is well damped in all cases. ∇

This example indicates that at least as far as parametric variations are concerned, the design based on a simple nominal model will give satisfactory control. The example also indicates that a controller with fixed parameters can be used in all cases. Notice however that we have not considered operating conditions in low gear and at low speed but cruise controllers are not used in these cases.

Unmodeled Dynamics

It is generally easy to investigate the effects of parametric variations. However, there are other uncertainties that also are important, as discussed at the end of Section 2.3. The simple model of the cruise control system only captures the dynamics of the forward motion of the vehicle and the torque characteristics of the engine and transmission. It does not, for example, include a detailed model of the engine dynamics (whose combustion processes are extremely complex) nor the slight delays that can occur in modern electronically-controlled engines (due to the processing time of the embedded computers). These neglected mechanisms are called *unmodeled dynamics*.

Unmodeled dynamics can be accounted for by developing a more complex model. Such models are commonly used for controller development but substan-

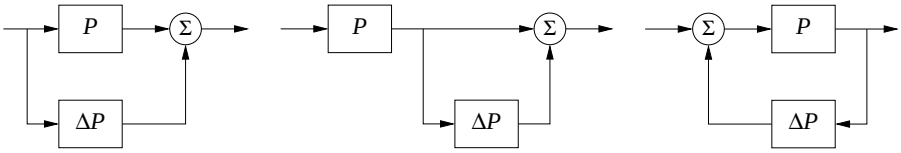

Figure 12.2: Unmodeled dynamics in linear systems. Uncertainty can be represented using additive perturbations (left), multiplicative perturbations (middle) or feedback perturbations (right). The nominal system is P and ΔP represents the unmodeled dynamics.

tial effort is required to develop the models. An alternative is to investigate if the closed loop system is sensitive to generic forms of unmodeled dynamics. The basic idea is to describe the "unmodeled" dynamics by including a transfer function in the system description whose frequency response is bounded, but otherwise unspecified. For example, we might model the engine dynamics in the cruise control example as a system that quickly provides the torque that is requested through the throttle, giving a small deviation from the simplified model, which assumed the torque response was instantaneous. This technique can also be used in many instances to model parameter variations, allowing a quite general approach to uncertainty management.

In particular we wish to explore if additional linear dynamics may cause difficulties. A simple way is to assume that the transfer function of the process is $P(s)+\Delta P(s)$ where $P(s)$ is the nominal simplified transfer function and $\Delta P(s)$ represents the unmodeled dynamics. This case is called *additive uncertainty*. Figure 12.2 shows some other cases to represent uncertainties in a linear system.

When are Two Systems Similar?

A fundamental issue in describing robustness is to determine when two systems are close. Given such a characterization, we can then attempt to describe robustness according to how close the actual system must be to the model in order to still achieve the desired levels of performance. This seemingly innocent problem is not as simple as it may appear. A naive idea is to say that two systems are close if their open loop responses are close. Even if this appears natural, there are complications, as illustrated by the following examples.

Example 12.2 Similar in open loop but large differences in closed loop
The systems with the transfer functions

$$P_1(s) = \frac{100}{s+1}, \qquad P_2(s) = \frac{100}{(s+1)(sT+1)^2}$$

have very similar open loop responses for small values of T, as illustrated in the top left corner of Figure 12.3a, where $T = 0.025$. The differences between the step responses are barely noticeable in the figure. The step responses with unit gain error feedback are shown in the bottom left figure. Notice that one closed loop system is stable and the other one is unstable. ∇

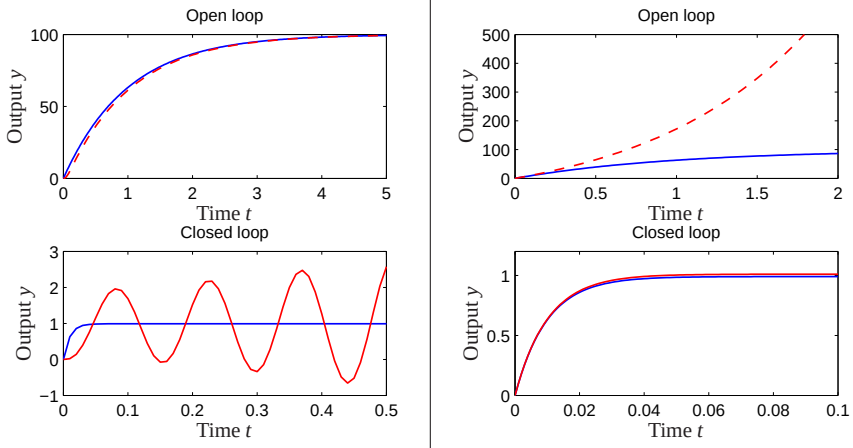

(a) Example 12.2 (b) Example 12.3

Figure 12.3: Determining when two systems are close. The plots on the left show the open and closed loop responses for two processes that have nearly identical step responses in open loop, but are very different in closed loop. The system on the right shows the opposite: the systems are different in open loop, but similar in closed loop.

Example 12.3 Different in open loop but similar in closed loop
Consider the systems

$$P_1(s) = \frac{100}{s+1}, \qquad P_2(s) = \frac{100}{s-1}.$$

The open loop responses are very different because P_1 is stable and P_2 is unstable, as shown in the top right plot in Figure 12.3. Closing a feedback loop with unit gain around the systems we find that the closed loop transfer functions are

$$T_1(s) = \frac{100}{s+101} \qquad T_2(s) = \frac{100}{s+99}$$

which are very close as is also shown in Figure 12.3b. ∇

These examples show that if our goal is to close a feedback loop it may be misleading to compare the open loop responses of the system. Inspired by these examples we will introduce a distance measure that is more appropriate for closed loop operation. Consider two systems with the rational transfer functions

$$P_1(s) = \frac{n_1(s)}{d_1(s)} \quad \text{and} \quad P_2(s) = \frac{n_2(s)}{d_2(s)},$$

where $n_1(s)$, $n_2(s)$, $d_1(s)$ and $d_2(s)$ are polynomials. Let

$$p(s) = d_1(s)n_2(-s) - n_1(s)d_2(-s)$$

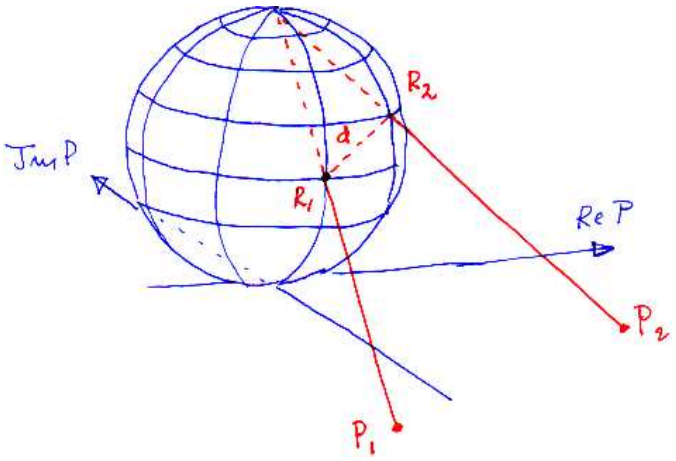

Figure 12.4: Geometric interpretation of the distance $d(P_1, P_2)$ between two transfer functions. At each frequency, the points on the Nyquist curve for P_1 and P_2 are projected onto a unit sphere of radius 1 sitting at the origin of the complex plane. The distance between the two systems is defined as the maximum distance between the points R_1 and R_2 over all frequencies.

and define the *chordal distance* between the transfer functions as

$$d_\nu(P_1, P_2) = \begin{cases} \sup\limits_{\omega} \dfrac{|P_1(i\omega) - P_2(i\omega)|}{\sqrt{(1+|P_1(i\omega)|^2)(1+|P_2(i\omega)|^2)}} & \text{if } p(s) \text{ has no RHP zeros} \\ 1 & \text{otherwise.} \end{cases} \tag{12.1}$$

The distance has a nice geometric interpretation, as shown in Figure 12.4, where the Nyquist plots of P_1 and P_2 are projected on the Riemann sphere. The Riemann sphere is located above the complex plane. It has diameter 1 and its south pole is at the origin of the complex plane. Points in the complex plane are projected onto the sphere by a line through the point and the north pole (Figure 12.4). The distance $d_\nu(P_1, P_2)$ is simply the shortest chordal distance between the projections of the Nyquist curves. The distance $d_\nu(P_1, P_2)$ is similar to $|P_1 - P_2|$ when the transfer functions are small, but very different when $|P_1|$ and $|P_2|$ are large. It is also related to the behavior of the systems under unit feedback as will be discussed in Section 12.5. Since the diameter of the Riemann sphere is 1, it follows that the distance is never larger than 1.

The *Vinnicombe metric* or the *ν-gap metric* (12.1) was introduced in [Vin01] and is a natural tool to compare the behavior of two systems under closed loop feedback. Vinnicombe also gave strong robustness results based on the metric. We illustrate by computing the metric for the systems in the previous examples.

Example 12.4 Vinnicombe metric for Examples 12.2 and 12.3
For the systems in Example 12.2 we have

$$n_1(s) = n_2(s) = 100, \qquad d_1(s) = s+1, \qquad d_2(s) = (s+1)(sT+1)^2$$

and hence

$$p(s) = d_1(s)n_2(-s) - n_1(s)d_2(-s) = 100s(sT^2 + T + 2).$$

This polynomial has no roots in the open right half plane and we can proceed to compute the norm (12.1) numerically, which for $T = 0.025$ gives $d(P_1, P_2) = 0.98$, a quite large value. To have a reasonable robustness the Vinnicombe recommended values less than 1/3.

For the system in Example 12.3 we have

$$n_1(s) = n_2(s) = 100, \qquad d_1(s) = s+1, \qquad d_2(s) = s-1$$

and

$$p(s) = d_1(s)n_2(-s) - n_1(s)d_2(-s) = 100(s+1-(-s+1)) = 200\,s.$$

This polynomial has no roots in the open right half plane and we can proceed to compute the norm (12.1) numerically, giving $d(P_1, P_2) = 0.02$, which is a very small value. This explains why both systems can be controlled well by the same controller. ∇

12.2 STABILITY IN THE PRESENCE OF UNCERTAINTY

Having discussed how to describe robustness, we now consider the problem of robust stability: when can we show that the stability of a system is robust with respect to process variations? This is an important question since the potential for instability is one of the main drawbacks of feedback. Hence we want to ensure that even if we have small inaccuracies in our model, we can still guarantee stability and performance.

Robust Stability Using Nyquist's Criterion

The Nyquist criterion provides a powerful and elegant way to study the effects of uncertainty for linear systems. A simple criterion is that the Nyquist curve is sufficiently far from the critical point -1. Recall that the shortest distance from the Nyquist curve to the critical point is $s_m = 1/M_s$ where M_s is the maximum of the sensitivity function and s_m the stability margin introduced in Section 9.3. The maximum sensitivity M_s or the stability margin s_m is thus a good robustness measure, as illustrated in Figure 12.5a.

We will now derive explicit conditions for permissible process uncertainties. Consider a stable feedback system with a process P and a controller C. If the process is changed from P to $P + \Delta P$, the loop transfer function changes from PC to $PC + C\Delta P$, as illustrated in Figure 12.5b. If we have a bound on the size of ΔP (represented by the dashed circle in the figure), then the system remains stable as long as the process variations never overlap the -1 point, since this leaves the number of encirclements of -1 unchanged.

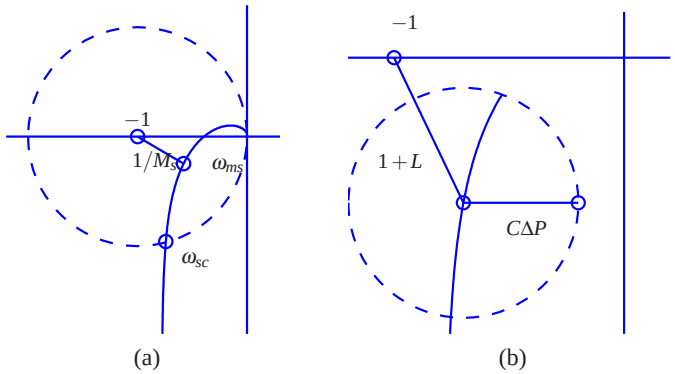

Figure 12.5: Robust stability using the Nyquist criterion. The left figure shows that the distance to the critical point $1/M_s$ is a robustness measure. The right figure shows the Nyquist curve of a nominal loop transfer function and its uncertainty caused by additive process variations ΔP.

Some additional assumptions are required for the analysis to hold. Most importantly, we require that the process perturbations ΔP be stable so that we do not introduce any new right half plane poles that would require additional encirclements in the Nyquist criterion. Also, we note that this condition is conservative: it allows for any perturbation that satisfies the given bounds, while in practice we may have more information about possible perturbations.

We now compute an analytical bound on the allowable process disturbances. The distance from the critical point -1 to the loop transfer function L is $|1+L|$. This means that the perturbed Nyquist curve will not reach the critical point -1 provided that

$$|C\Delta P| < |1+L|,$$

which implies

$$|\Delta P| < \left|\frac{1+PC}{C}\right| \qquad \text{or} \qquad \left|\frac{\Delta P}{P}\right| < \frac{1}{|T|}. \tag{12.2}$$

This condition must be valid for all points on the Nyquist curve, i.e pointwise for all frequencies. The condition for robust stability can thus be written as

$$\left|\frac{\Delta P(i\omega)}{P(i\omega)}\right| < \frac{1}{|T(i\omega)|} \qquad \text{for all } \omega \geq 0. \tag{12.3}$$

This condition allows us to reason about uncertainty without exact knowledge of the process perturbations. Namely, we can verify stability for *any* uncertainty ΔP that satisfies the given bound. From an analysis perspective, this gives us a measure of the robustness for a given design. Conversely, if we require robustness of a given level, we can attempt to choose our controller C such that the desired level of robustness is available (by asking T to be small) in the appropriate frequency bands.

The formula given by equation (12.3) is one of the reasons why feedback systems work so well in practice. The mathematical models used to design control

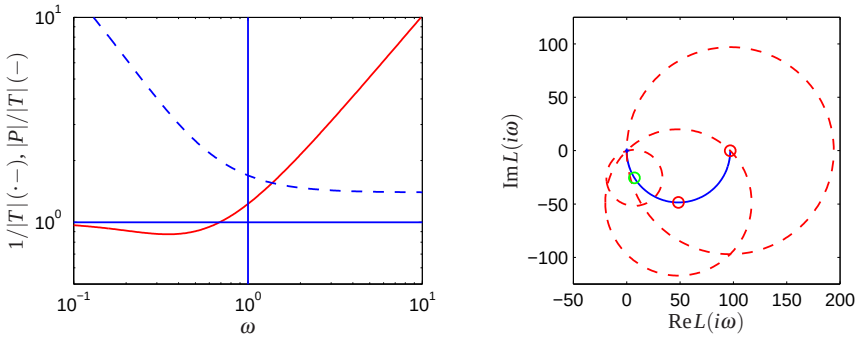

Figure 12.6: Robustness for a cruise controller. The left figure shows the maximum relative error ($1/|T|$, dot-dashed) and absolute error ($|P|/|T|$, solid) for the process uncertainty ΔP. The Nyquist curve is shown in the right figure, as a solid line. The dashed circles show permissible perturbations in the process dynamics, $|\Delta P| = |P|/|T|$, at the frequencies $\omega = 0$, 0.0142 and 0.05.

system are often strongly simplified. There may be model errors and the properties of a process may change during operation. Equation (12.3) implies that the closed loop system will at least be stable for substantial variations in the process dynamics.

It follows from equation (12.3) that the variations can be large for those frequencies where T is small and that smaller variations are allowed for frequencies where T is large. A conservative estimate of permissible process variations that will not cause instability is given by

$$\left|\frac{\Delta P(i\omega)}{P(i\omega)}\right| < \frac{1}{M_t},$$

where M_t is the largest value of the complementary sensitivity

$$M_t = \sup_\omega |T(i\omega)| = \left\|\frac{PC}{1+PC}\right\|_\infty. \tag{12.4}$$

The value of M_t is influenced by the design of the controller. For example, it is shown in Exercise 12.1 that if $M_t = 2$ then pure gain variations of 50% or pure phase variations of 30° are permitted without making the closed loop system unstable.

Example 12.5 Cruise control

Consider the cruise control system discussed in Section 3.1. The model of the car in fourth gear at speed 25 m/s is

$$P(s) = \frac{1.38}{s+0.0142},$$

and the controller is a PI controller with gains $k = 0.72$ and $k_i = 0.18$. Figure 12.6 plots the allowable size of the process uncertainty using the bound in equation (12.3). At low frequencies, $T(0) = 1$ and so the perturbations can be

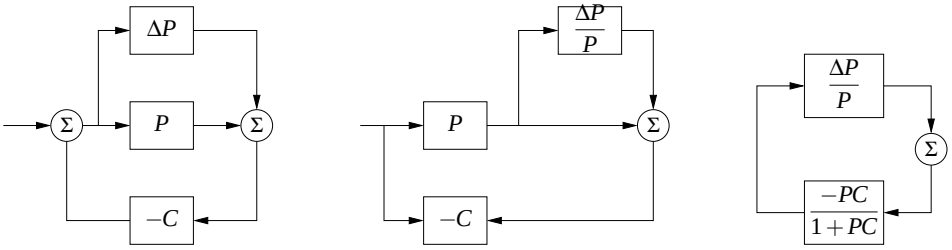

Figure 12.7: Illustration of robustness to process perturbations. A system with additive uncertainty (left) can be manipulated via block diagram algebra (center) to isolate the uncertainty in a manner that allows application of the small gain theorem (right)

as large as the original process ($|\Delta P/P| < 1$). The complementary sensitivity has its maximum $M_t = 1.14$ at $\omega_{mt} = 0.35$ and hence this gives the minimum allowable process uncertainty, with $|\Delta P/P| < 0.87$ or $|\Delta P| < 3.47$. Finally, at high frequencies $T \to 0$ and hence the relative error can get very large. For example, at $\omega = 5$ we have $|T(i\omega)| = 0.195$ which means that the stability requirement is $|\Delta P/P| < 5.1$. The analysis clearly indicates that the system has good robustness and that the high frequency properties of the transmission system are not important for the design of the cruise controller.

Another illustration of the robustness of the system is given in the right diagram of Figure 12.6, which shows the Nyquist curve of the transfer function of the process and the uncertainty bounds $\Delta P = |P|/|T|$ for a few frequencies. Note that the controller can tolerate large amounts of uncertainty and still maintain stability of the closed loop. ∇

The situation illustrated in the previous example is typical of many processes: moderately small uncertainties are only required around the gain crossover frequencies, but large uncertainties can be permitted at higher and lower frequencies. A consequence of this is that a simple model that describes the process dynamics well around the crossover frequency is often sufficient for design. Systems with many resonance peaks are an exception to this rule because the process transfer function for such systems may have large gains also for higher frequencies, as shown for instance in Example 9.9.

Notice that the results we have given can be conservative. Referring to Figure 12.5, the critical perturbations, which were the basis for our analysis, are in the direction towards the critical point. It is possible to have much larger perturbations in the opposite direction.

The robustness result given by equation (12.3) can be given another interpretation by using the small gain theorem, Theorem 9.4 on page 284. To apply the theorem we start with block diagrams of a closed loop system with a perturbed process and we make a sequence of transformations of the block diagram which isolates the block which represents the uncertainty, as shown in Figure 12.7. The result is the two-block interconnection shown in Figure 12.7c which has the loop

Table 12.1: Conditions for robust stability for different types of uncertainty.

Process	Type	Robust Stability
$P+\Delta P$	Additive	$\|CS\Delta P\|_\infty < 1$
$P(1+\Delta P)$	Multiplicative	$\|S\Delta P\|_\infty < 1$
$P/(1+\Delta P\cdot P)$	Feedback	$\|PS\Delta P\|_\infty < 1$

transfer function

$$L = \frac{PC}{1+PC}\frac{\Delta P}{P} = T\frac{\Delta P}{P}.$$

Equation (12.3) implies that the largest loop gain is less than one and hence the systems is stable via the small gain theorem.

The small gain theorem can be used to check robust stability for uncertainty in a variety of other situations. Table 12.1 summarizes a few of the common cases; the proofs (all via the small gain theorem) are left as exercises.

The following example illustrates that it is possible to design systems that are robust to parameter variations.

Example 12.6 Bode's loop transfer function

A major problem in design of electronic amplifiers was to obtain a closed loop system that was insensitive to changes in the gain of the electronic components. Bode found that the loop transfer function $L(s) = ks^n$, with $-5/3 \le n \le -1$ was an ideal loop transfer function. Figure 12.8a shows that the Bode and Nyquist plots of the loop transfer function. Notice that the gain curve is a straight line with slope n and that the phase is constant $\angle L(i\omega) = n\pi/2$. The phase margin is thus constant $\varphi_m = -sin^{-1}(n\pi/2)$ for all values of controller gain k. The Nyquist curve is a straight line from the origin. The transfer function cannot be realized with

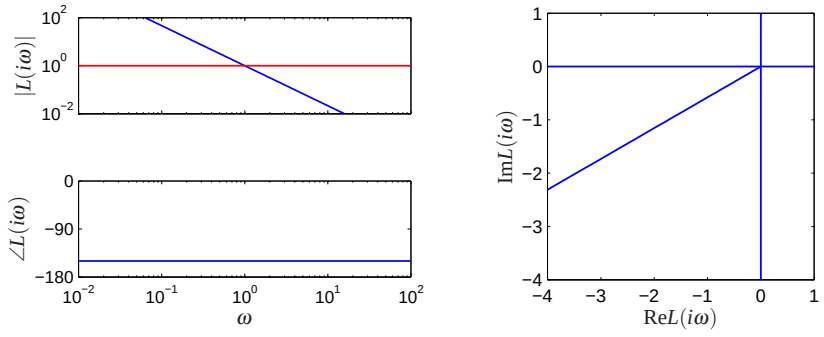

(a) (b)

Figure 12.8: Bode's ideal loop transfer function. Bode and Nyquist plots are shown for Bode's ideal loop transfer function $L(s) = ks^n$, for $k = 1$ and $n = 5/3$.

physical components, but it can be approximated over a given frequency range with a rational function that can be implemented. An operational amplifier circuit that has the approximate transfer function $G(s) = k/(s+a)$ is a realization of Bode's ideal transfer function with $n = 1$, as described in Example 8.3. Designers of operational amplifiers make great effort to make the approximation valid over a wide frequency range. ∇

Youla Parameterization

Since stability is such an essential property it is useful to characterize all controllers that will stabilize a given process. Consider a stable process with a rational transfer function P. A system with the complementary sensitivity function T can be obtained by feedforward control with the stable transfer function Q if

$$T = PQ \tag{12.5}$$

Notice that T must have the same right half plane zeros as P since Q is stable. Now assume that we want to obtain the complementary transfer function T by using unit feedback with the controller C. Since $T = PC/(1+PC) = PQ$ we find that the controller transfer function is

$$C = \frac{Q}{1-QP}. \tag{12.6}$$

A straightforward calculation gives

$$\frac{1}{1+PC} = 1-T, \quad \frac{P}{1+PC} = P-PT, \quad \frac{C}{1+PC} = Q, \quad \frac{PC}{1+PC} = T$$

which are all stable. It can be shown that all stabilizing controllers for a stable process $P(s)$ are given by equation (12.6) for some stable $Q(s)$. Equation (12.6) is called a *Youla parameterization*: it characterizes all controllers that stabilize a stable process. The parameterization is illustrated by the block diagrams in Figure 12.9a.

A similar characterization can be obtained for unstable systems. Consider a process with a rational transfer function $P(s) = a(s)/b(s)$ where $a(s)$ and $b(s)$ are polynomials. By introducing a stable polynomial $c(s)$ we can write

$$P(s) = \frac{a(s)}{b(s)} = \frac{A(s)}{B(s)},$$

where $A(s) = a(s)/c(s)$ and $B(s) = b(s)/c(s)$ are stable rational functions. We have

$$\frac{1}{1+PC_0} = \frac{AF_0}{AF_0+BG_0} = S_0 \qquad \frac{P}{1+PC_0} = \frac{BF_0}{AF_0+BG_0} = PS_0$$

$$\frac{C_0}{1+PC_0} = \frac{AG_0}{AF_0+BG_0} = CS_0 \qquad \frac{PC_0}{1+PC_0} = \frac{BG_0}{AF_0+BG_0} = T_0$$

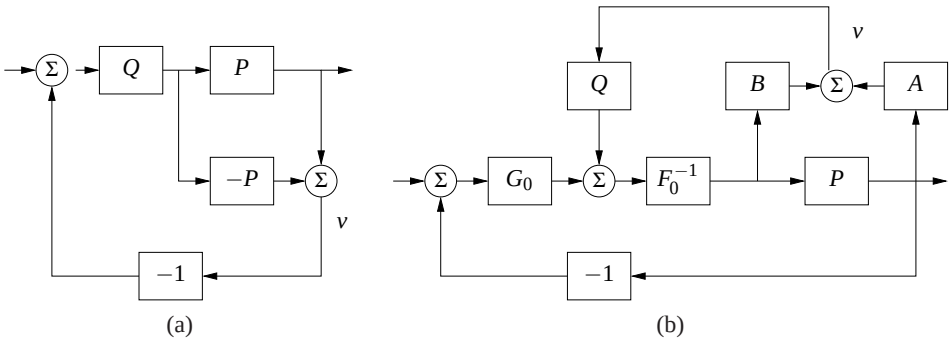

Figure 12.9: Youla parameterization. Block diagrams of Youla parameterizations for a stable system (left) and an unstable system (right). Notice that the signal v is zero in steady state.

Since C is a stabilizing controller the function $AF_0 + BG_0$ must have all its zeros in the left half plane. All stabilizing controllers are now given by

$$C = \frac{G_0 + QA}{F_0 - QB} \tag{12.7}$$

and we have

$$\frac{1}{1+PC} = \frac{A(F_0 - QG)}{AF_0 + BG_0} \qquad \frac{P}{1+PC} = \frac{BF_0 - QB^2}{AF_0 + BG_0}$$
$$\frac{C}{1+PC} = \frac{AG_0 + QA^2}{AF_0 + BG_0} \qquad \frac{PC}{1+PC} = \frac{AF_0 + BG_0}{AF_0 + BG_0}.$$

Equation (12.7) reduces to equation (12.6) for $F_0 = 1$ and $G_0 = 0$. A block diagram is shown in Figure 12.9b. Notice that the transfer function Q appears affinely in the expressions for the Gang of Four, which is very useful if we want to determine the transfer function Q to obtain specific properties.

12.3 PERFORMANCE IN THE PRESENCE OF UNCERTAINTY

So far we have investigated the risk for instability and robustness to process uncertainty. We will now explore how responses to load disturbances, measurement noise and command signal following are influenced by process variations. To do this we will analyze the system in Figure 12.10, which is identical to the basic feedback loop analyzed in Chapter 11.

Disturbance Attenuation

The sensitivity function S gives a rough characterization of the effect of feedback on disturbances as was discussed in Section 11.1. A more detailed characterization

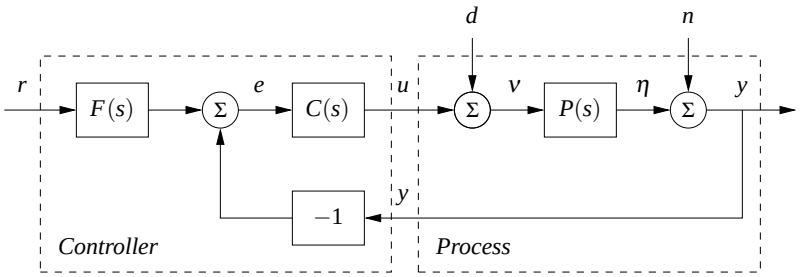

Figure 12.10: Block diagram of a basic feedback loop. The external signals are the command signal r, the load disturbance d and the measurement noise n. The process output is y and the control signal is u. The process P may include unmodeled dynamics, such as additive perturbations.

is given by the transfer function from load disturbances to process output:

$$G_{yd} = \frac{P}{1+PC} = PS. \tag{12.8}$$

Load disturbances typically have low frequencies and it is therefore important that the transfer function is small for low frequencies. For processes with constant low frequency gain and a controller with integral action we have $G_{yd} \approx s/k_i$. Integral gain k_i is thus a simple measure of attenuation of load disturbances.

To find how the transfer function G_{yd} is influenced by small variations in the process transfer function we write P as $P+\Delta P$ and try to find the corresponding ΔG_{yd}. If the perturbations are sufficiently small, we can show that

$$\begin{aligned} G_{yd} + \Delta G_{yd} &\approx \frac{P+\Delta P}{1+(P+\Delta P)C} \approx \frac{P}{1+PC} + \frac{\Delta P}{1+PC} \\ &= PS + S\Delta P = G_{yd} + \frac{G_{yd}}{P}\Delta P, \end{aligned}$$

where we have ignored terms that are quadratic and higher in ΔP. It follows that

$$\frac{dG_{yd}}{G_{yd}} = S\frac{dP}{P}, \tag{12.9}$$

where we write dG and dP as a reminder that this expression holds for small variations. The response to load disturbances is thus insensitive to process variations for frequencies where $|S(i\omega)|$ is small, i.e. for those frequencies where load disturbances are important.

A drawback with feedback is that the controller feeds measurement noise into the system. In addition to the load disturbance rejection, it is thus also important that the control actions generated by measurement noise are not too large. It follows from Figure 12.10 that the transfer function G_{un} from measurement noise to controller output is given by

$$G_{un} = -\frac{C}{1+PC} = -\frac{T}{P}. \tag{12.10}$$

Since measurement noise typically has high frequencies, the transfer function G_{un} should not be too large for high frequencies. The loop transfer function PC is typically small for high frequencies, which implies that $G_{un} \approx C$ for large s. To avoid injecting too much measurement noise it is therefore important that $C(s)$ is small for large s. This property is called high frequency roll-off. An example is filtering of the measured signal in a PID controller to reduce injection of measurement noise; see Section 10.5.

To find how the transfer function G_{un} is influenced by small variations in the process transfer function we expand equation (12.10) and obtain the first order variations, which gives

$$\frac{dG_{un}}{G_{un}} = T\frac{dP}{P}. \tag{12.11}$$

Note that this same expression can be also be obtained by differentiation of equation (12.10):

$$\frac{dG_{un}}{dP} = \frac{d}{dP}\left(-\frac{C}{1+PC}\right) = \frac{C}{(1+PC)^2}C = T\frac{G_{un}}{P}.$$

Measurement noise typically has high frequencies. Since the complementary sensitivity function is also small for high frequencies, we find that process uncertainty has little influence on the transfer function G_{un} for frequencies where measurements are important.

Command Signal Following

The transfer function from reference to output is given by

$$G_{yr} = \frac{PCF}{1+PC} = TF, \tag{12.12}$$

which contains the complementary sensitivity function. To see how variations in P affect the performance of the system, we differentiate equation (12.12) with respect to the process transfer function:

$$\frac{dG_{yr}}{dP} = \frac{CF}{1+PC} - \frac{PCFC}{(1+PC)^2} = \frac{CF}{(1+PC)^2} = S\frac{G_{yr}}{P}.$$

and it follows that

$$\frac{dG_{yr}}{G_{yr}} = S\frac{dP}{P}. \tag{12.13}$$

The relative error in the closed loop transfer function thus equals the product of the sensitivity function and the relative error in the process. In particular, it follows from equation (12.13) that the relative error in the closed loop transfer function is small when the sensitivity is small. This is one of the useful properties of feedback.

As in the last section, there are some mathematical assumptions that are required in order for the analysis presented here to hold. As already stated, we require that the perturbations ΔP be small (as indicated by writing dP). Secondly, we require that the perturbations be stable, so that we do not introduce any new

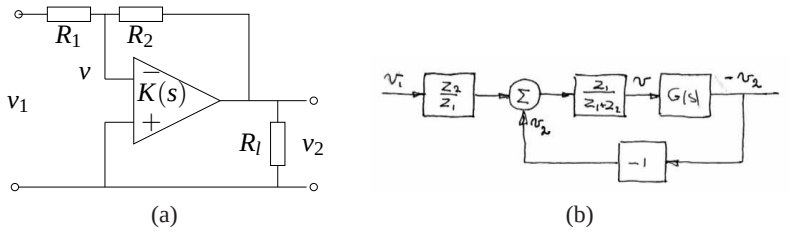

(a) (b)

Figure 12.11: Op amp with uncertain dynamics. The op amp circuit (right) is modeled using $G(s)$ to capture its dynamic properties and includes a load at the output. The block diagram (right) shows the input/output relationships. The load is represented as a disturbance d applied at the output of $G(s)$.

right half plane poles that would require additional encirclements in the Nyquist criterion. Also, as before this condition is conservative: it allows for any perturbation that satisfies the given bounds, while in practice the perturbations may be more restricted.

Example 12.7 Op amp

To illustrate the use of these tools, consider the performance of an op amp based amplifier, as shown in Figure 12.11. We wish to analyze the performance of the amplifier in the presence of uncertainty in the dynamic response of the op amp and changes in the loading on the output. We model the system using the block diagram in Figure 12.11b, which is based on the derivation in Example 9.1.

Consider first the effect of unknown dynamics for the operational amplifier. If we model the dynamics of the op amp as

$$v_{\text{out}} = G(s)(v_+ - v_-)$$

then transfer function for the overall circuit is given by

$$H_{v_2 v_1} = -\frac{R_2}{R_1}\frac{G(s)}{G(s) + R_2/R_1 + 1}.$$

We see that if $G(s)$ is large over the desired frequency range, then the closed loop system is very close to the ideal response R_2/R_1. We can make this more explicit by assuming that $G(s)$ has the form

$$G(s) = \frac{b}{s+a}, \qquad \frac{a - a_{\text{nom}}}{a_{\text{nom}}} < \delta, \qquad b_{\min} \le b \le b_{\max}.$$

The term a is the bandwidth of the amplifier and b is the bandwidth product for the amplifier as discussed in Example 8.3.

The sensitivity function and complementary sensitivity function for the nominal dynamics are given by

$$S = \frac{s+a}{s+a+\alpha b} \qquad T = \frac{\alpha b}{s+a+\alpha b},$$

where $\alpha = R_2/R_1$. The sensitivity function around the nominal values tell us how

the tracking response response varies as a function of process perturbations:

$$\frac{dG_{yr}}{G_{yr}} = S\frac{dP}{P}$$

We see that for low frequencies, where S is small, variations in the bandwidth or the gain-bandwidth product will have relatively little effect on the performance of the amplifier (under the assumption that b is sufficiently large.

To model the effects of unknown load, we consider the addition of a disturbance at the output of the system, as shown in Figure 12.11b. This disturbance represents changes in the output voltage to due loading effects. The transfer function $G_{yd} = S$ gives the response of the output to the load disturbance and we see that if S is small then we are able to reject such disturbances. The sensitivity of G_{yd} to perturbations in the process dynamics can be computed by taking the derivative of G_{yd} with respect to P:

$$\frac{dG_{yd}}{dP} = \frac{-C}{(1+PC)^2} = \frac{T}{P}G_{yd} \qquad \Longrightarrow \qquad \frac{dG_{yd}}{G_{yd}} = T\frac{dP}{P}.$$

Thus we see that the relative changes in the disturbance rejection are roughly the same as the process perturbations at low frequency (when T is approximately 1) and drop off at higher frequencies. However, it is important to remember that G_{yd} itself is small at low frequency, and so these variations in relative performance may not be an issue in many applications. ∇

12.4 ROBUST POLE PLACEMENT

In Chapters 6 and 7 we saw how to design controllers by setting the locations of the eigenvalues of the closed loop system. If we analyze the resulting system in the frequency domain, the closed loop eigenvalues correspond to the poles of the closed loop transfer function and hence these methods are often referred to as design by "pole placement".

The design methods we used in the state space, as with many methods developed for control system design, did not explicitly take robustness into account. In such cases it is essential to always investigate the robustness because there are seemingly reasonable designs that give controllers with poor robustness. We illustrate this by analyzing controllers designed by state feedback and observers. The closed loop poles can be assigned to arbitrary locations if the system is observable and reachable. However if we want to have a robust closed loop system, the poles and zeros of the process impose severe restrictions on the location of the closed loop poles. Some examples are first given; based on analysis of these examples we then describe design rules for robust pole placement.

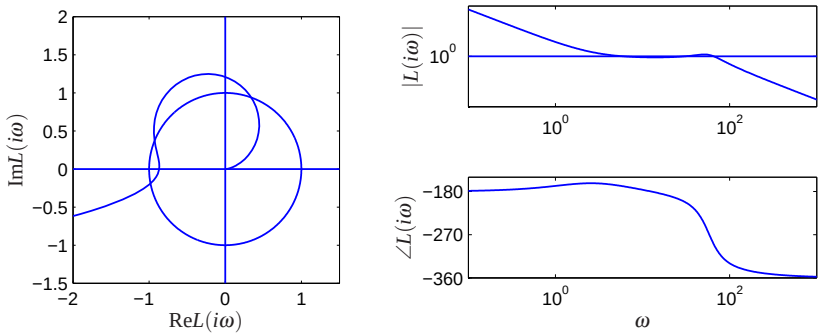

Figure 12.12: Observer-based control of steering. The Nyquist plot (left) and Bode plot (right) of the loop transfer function for vehicle steering with a controller based on state feedback and an observer. The controller provides stable operation, but with very low gain and phase margin.

Slow Stable Zeros

We will first explore the effects of slow stable zeros, and we begin with a simple example.

Example 12.8 Vehicle steering
Consider the linearized model for vehicle steering in Example 8.6, which has the transfer function

$$P(s) = \frac{0.5s+1}{s^2}.$$

A controller based on an observer and state feedback with the closed loop poles given by $\omega_c = 1$, $\zeta_c = 0.707$, $\omega_o = 2$ and $\zeta_o = 0.707$ was designed in Example 7.3. Assume that we want a faster closed loop system and choose $\omega_c = 10$, $\zeta_c = 0.707$, $\omega_o = 20$ and $\zeta_o = 2$. A pole placement design gives state feedback gain $k_1 = 100$ and $k_2 = -35.86$ and observer gains $l_1 = 28.28$ and $l_2 = 400$. The controller transfer function is

$$C(s) = \frac{-11516s+40000}{s^2+42.4s+6657.9}.$$

Figure 12.12 shows Nyquist and Bode plots of the loop transfer function. The Nyquist plot indicates that the robustness is poor since the loop transfer function is very close to the critical point -1. The phase margin is only 7°. This also shows up in the Bode plot where the gain curve hovers around the value 1 and the phase curve is close to 180° for a wide frequency range.

More insight is obtained by analyzing the sensitivity functions, shown by full lines in Figure 12.13. The maximum sensitivities are $M_s = 13$ and $M_t = 12$, indicating that the system has poor robustness.

At first sight it is surprising that a controller where the nominal system has well damped poles and zeros is so sensitive to process variations. We have an indication that something is unusual because the controller has a zero $s = 3.9$ in the right half plane. To understand what happens we will investigate the reason for the peaks of

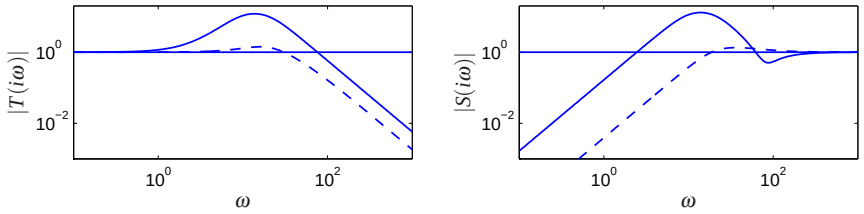

Figure 12.13: Sensitivity functions for observer-based control of vehicle steering. The complementary sensitivity function (left) and sensitivity function (right) for the original controller with $\omega_c = 10$, $\zeta_c = 0.707$, $\omega_o = 20$, $\zeta_o = 0.707$ (solid) and the improved controller with $\omega_c = 10$, $\zeta_c = 2.6$ (dashed).

the sensitivity functions.

Let the transfer functions of the process and the controller be

$$P(s) = \frac{n_p(s)}{d_p(s)} \qquad C(s) = \frac{n_c(s)}{d_c(s)},$$

where $n_p(s)$, $n_c(s)$, $d_p(s)$ and $d_c(s)$ are the numerator and denominator polynomials. The complementary sensitivity function is

$$T(s) = \frac{PC}{1+PC} = \frac{n_p(s)n_c(s)}{d_p(s)d_c(s)+n_p(s)n_p(s)}.$$

$T(s)$ is 1 for low frequency and starts to increase at its first zero, which is the process zero at $s = 2$. It increases further at the controller zero at $s = 3.9$ and it does not start to decrease until the closed loop poles appear at $\omega_c = 10$ and $\omega_o = 20$. We can thus conclude that there will be a peak in the complementary sensitivity function. The magnitude of the peak depends on the ratio of the zeros and the poles of the transfer function.

The peak of the complementary sensitivity function can be avoided by assigning a closed loop zero close to the slow process zero. We can achieve this by choosing $\omega_c = 10$ and $\zeta_c = 2.6$ which gives the closed loop poles at $s = -2$ and $s = -50$. The controller transfer function then becomes

$$C(s) = \frac{3628s + 40000}{s^2 + 80.28s + 156.56} = 3628\,\frac{s+11.02}{(s+2)(s+78.28)}$$

The sensitivity functions are shown in dashed lines in Figure 12.13. The controller gives the maximum sensitivities $M_s = 1.34$ and $M_t = 1.41$, which gives much better robustness. Notice that the controller has a pole at $s = -2$ that cancels the slow process zero. The design can also be done simply by canceling the slow, stable process zero and designing the system for the simplified system. ∇

One lesson from the example is that it is necessary to choose closed loop poles that are equal to or close to slow, stable process zeros. Another lesson is that slow, unstable process zeros impose limitations on the achievable bandwidth, as was already noted in Section 11.5.

Fast Stable Process Poles

The next example shows the effect of fast stable poles.

Example 12.9 Fast system poles
Consider a PI controller for a first order system, where the process and the controller have the transfer functions

$$P(s) = \frac{b}{s+a} \qquad C(s) = k + \frac{k_i}{s}.$$

The loop transfer function is

$$L(s) = \frac{b(ks+k_i)}{s(s+a)}$$

and the closed loop characteristic polynomial is

$$s(s+a) + b(ks+k_i) = s^2 + (a+bk)s + k_i.$$

If we let the desired closed loop characteristic polynomial be

$$(s+p_1)(s+p_2),$$

we find that the controller parameters are given by

$$k = \frac{p_1+p_2-a}{b} \qquad k_i = \frac{p_1 p_2}{b}.$$

The sensitivity functions are then

$$S(s) = \frac{s(s+a)}{(s+p_1)(s+p_2)} \qquad T(s) = \frac{(p_1+p_2-a)s+p_1p_2}{(s+p_1)(s+p_2)}.$$

Assume that the process pole a is much larger than the closed loop poles p_1 and p_2, say $p_1 < p_2 < a$. Notice that the proportional gain is negative and that the controller has a zero in the right half plane if $a > p_1 + p_2$, an indication that the system has bad properties.

Next consider the sensitivity function, which is 1 for high frequencies. Moving from high to low frequencies we find that the sensitivity increases at the process pole $s = a$. The sensitivity does not decrease until the closed loop poles are reached, resulting in a large sensitivity peak that is approximately a/p_2. The magnitude of the sensitivity function is shown in Figure 12.14 for $a = b = 1$, $p_1 = 0.05$, $p_2 = 0.2$. Notice the high sensitivity peak. For comparison we have also shown the gain curve for the case when the closed loop poles are faster than the than the process pole ($p_1 = 5$, $p_2 = 20$). The problem with the poor robustness can be avoided by choosing one closed loop pole equal to the process pole, i.e. $p_2 = a$. The controller gains then become

$$k = \frac{p_1}{b} \qquad k_i = \frac{ap_1}{l},$$

which means that the fast process pole is canceled by a controller zero. The loop

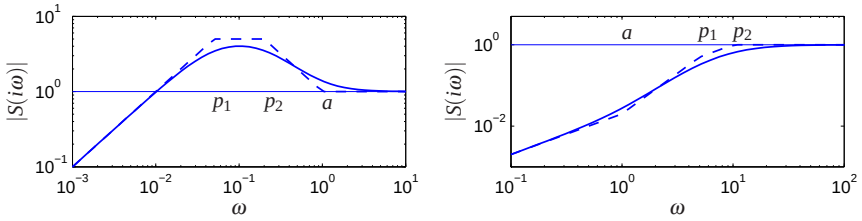

Figure 12.14: Gain curves for Bode plots of the sensitivity function S for designs with $p_1 < p_2 < a$ (left) and $a < p_1 < p_2$ (right). The full lines are the true sensitivities and the dashed lines are the asymptotes

transfer function and the sensitivity functions are

$$L(s) = \frac{bk}{s} \qquad S(s) = \frac{s}{s+bk} \qquad T(s) = \frac{bk}{s+bk}.$$

The maximum sensitivities are less than 1 for all frequencies. Notice that this is possible because the process transfer function goes to zero as s^{-1}. ∇

Design Rules for Pole-Placement

Based on the insight gained from the examples it is now possible to obtain design rules that give designs with good robustness. Consider the expression (12.8) for the complementary sensitivity function, repeated here:

$$M_t = \sup_\omega |T(i\omega)| = \left\| \frac{PC}{1+PC} \right\|_\infty.$$

Let ω_{gc} be the desired gain crossover frequency. Assume that the process has zeros that are slower than ω_{gc}. The complementary sensitivity function is 1 for low frequencies and it increases for frequencies close to the process zeros unless there is a closed loop pole in the neighborhood. To avoid large values of the complementary sensitivity function we find that the closed loop system should have poles close to or equal to the slow stable zeros. This means that slow stable zeros should be canceled by controller poles. Since unstable zeros cannot be canceled, the presence of slow unstable zeros means that achievable gain crossover frequency must be smaller than the slowest unstable process zero.

Now consider process poles that are faster than the desired gain crossover frequency. Consider the expression for the maximum of the sensitivity function.

$$M_s = \sup_\omega |S(i\omega)| = \left\| \frac{1}{1+PC} \right\|_\infty.$$

The sensitivity function is 1 for high frequencies. Moving from high to low frequencies the sensitivity function increases at the fast process poles. Large peaks can result unless there are closed loop poles close to the fast process poles. To avoid large peaks in the sensitivity the closed loop system should have poles that match the fast process poles. This means that the controller should cancel the fast

process poles by controller zeros. Since unstable modes cannot be canceled, the presence of a fast unstable pole implies that the gain crossover frequency must be sufficiently large.

To summarize, we obtain the following simple design rule: slow stable process zeros should be matched slow closed loop poles and fast stable process poles should be matched by fast process poles. Slow unstable process zeros and fast unstable process poles impose severe limitations.

Example 12.10 Nanopositioner
A simple nanopositioner was explored in Example 9.9 where it was shown that the system could be controlled using a an integrating controller. The performance of the closed loop was poor, because the gain crossover frequency was limited to $2\zeta_0\omega_0(1-s_m)$. In Exercise **??** it was also shown that little could be gained by adding proportional action. To obtain improved performance we will therefore us a PID controller. For modest increases we will use the design rule derived in Example 12.9 that fast stable process poles should be canceled by controller zeros. The controller transfer function should thus be chosen as

$$C(s) = \frac{k_d s^2 + k_p s + k_i}{s} = \frac{k_i}{s}\frac{s^2 + 2\zeta s + a^2}{a^2} \tag{12.14}$$

which gives $k_p = 2\zeta k_i/a$ and $k_d = k_i/a^2$.

Figure 12.15 shows the gain curves for the Gang of Four for a system designed with $k_i = 0.5$. A comparison with Figure 9.12 on page 279 shows that the bandwidth is increased significantly from $\omega_{gc} = 0.01$ to $\omega_{gc} = k_i = 0.5$. Since the process pole is canceled the system will however still be very sensitive to load disturbances with frequencies close to the resonant frequency. The gain curve of $CS(s)$ has a dip or a notch at the resonance frequency, which implies that the controller gain is very low for frequencies around the resonance. The gain curve also shows that the system is very sensitive to high frequency noise. The system will likely be unusable because the gain goes to infinity for high frequencies.

This can easily be remedied by modifying the controller to

$$C(s) = \frac{k_i}{s}\frac{s^2 + 2\zeta s + a^2}{a^2(1 + sT_f + (sT_f)^2/2)}, \tag{12.15}$$

which has high-frequency roll-off. Selection of the constant T_f of the filter is a compromise between attenuation of high frequency measurement noise and robustness. A large value of T_f reduces effects of sensor noise significantly but it also reduces the stability margin. A bit of experimentation using the Gang of Four gives $T_f = 0.75$ as a good compromise and the curves shown in full lines in Figure 12.15. The curves for $CS(s)$ shown that the effect of high-frequency roll-off due to filtering is quite dramatic. Notice that the poor attenuation of disturbances with frequencies close to the resonance are not visible in the sensitivity function because of the cancellation of poles and zeros.

The designs thus far have the drawback that load disturbances with frequencies close to the resonance are not attenuated. We will now consider a design that

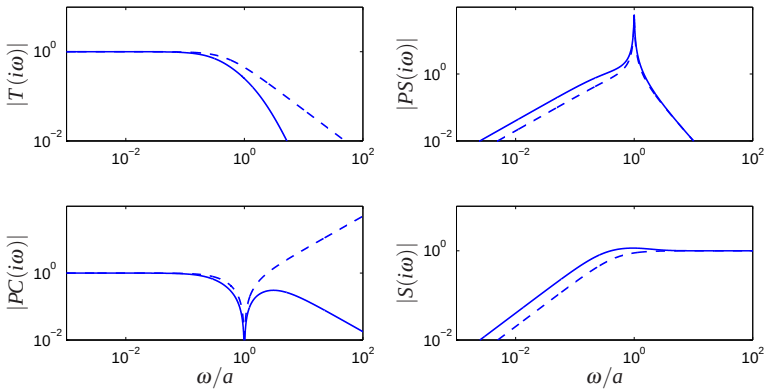

Figure 12.15: Nanopositioner control via cancellation of the fast process pole. Gain curves for the Gang of Four for PID control with second order filtering (12.15) are shown in full and the dashed lines show results for an ideal PID controller without filtering (12.14).

that actively attenuates the poorly damped modes. We will start with an ideal PID controller where the design can be done analytically and we will add high frequency roll-off. The loop transfer function obtained with this controller is

$$L(s) = \frac{k_d s^2 + k_p s + k_i}{s(s^2 + 2\zeta a s + a^2)}. \tag{12.16}$$

The closed loop system is of third order and its characteristic polynomial is

$$s^3 + (k_d a^2 + 2\zeta a)s^2 + (k_p + 1)a^2 s + k_i a^2. \tag{12.17}$$

A general third order polynomial can be parameterized as

$$(s + \alpha_0\omega_0)(s^2 + 2\zeta_0\omega_0 s + \omega_0^2) = s^3 + (\alpha_0 + 2\zeta_0)\omega_0 s^2 + (1 + 2\alpha_0\zeta_0)\omega_0^2 s + \alpha_0\omega_0^3. \tag{12.18}$$

Parameters α_0 and ζ_0 give the configuration of the poles and parameter ω_0 their magnitudes and therefore also the bandwidth of the system.

Identification of coefficients of equal powers of s in equations (12.17) and (12.18) gives the following equations for the controller parameters

$$\begin{aligned} k_d a^2 + 2\zeta a &= (\alpha_0 + 2\zeta_0)\omega_0 \\ a^2(k_p + 1) &= (1 + 2\alpha_0\zeta_0)\omega_0^2 \\ a^2 k_i &= \alpha_0\omega_0^3. \end{aligned} \tag{12.19}$$

To obtain a design with active damping it is necessary that the closed loop bandwidth is at least as fast as the oscillatory modes. Adding high frequency roll-off the controller becomes

$$C(s) = \frac{k_d s^2 + k_p s + k}{s(1 + sT_f + (sT_f)^2/2)}. \tag{12.20}$$

The value $T_f = T_d/10 = k_d/(10k)$ is a good value of the filtering time constant.

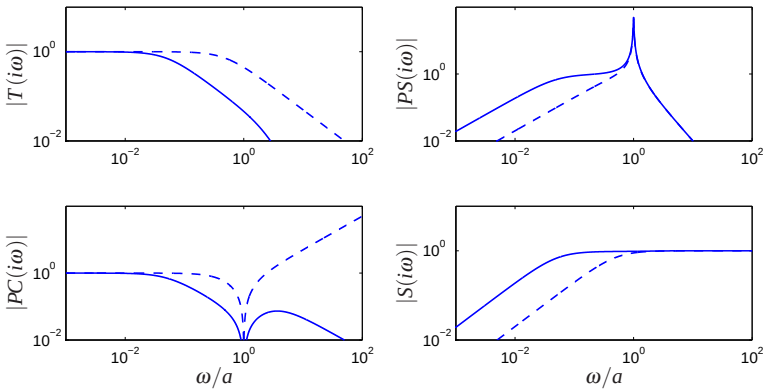

Figure 12.16: Nanopositioner control using active damping. Gain curves for the Gang of Four for PID control using the controller (12.16). The controller has high frequency roll-off and has been designed to give active damping of the oscillatory mode. The different curves correspond to different choices of magnitudes of the poles, parameterized by ω_0 in equation (12.16).

In Figure 12.16 we show the gain curves of the Gang of Four for designs with $\zeta = 0.707$, $\alpha_0 = 2$ and $\omega_0 = a$, $2a$ and $4a$. The figure shows that the largest values of the sensitivity function and the complementary sensitivity function are small. The gain curve for $PS(s)$ shows that load disturbances are now well attenuated over the whole frequency range. The gain curve for CS shows that large control signals are required to provide active damping. The high values of $CS(i\omega)$ for high frequencies also show that low noise sensors and actuators with a wide range are required. The largest gains for $CS(s)$ are 60 , 262 and 1074 for $\omega_0 = a$, $2a$ and $4a$ respectively. The high frequency gain of the controller thus increases dramatically with the value of ω_0. A comparison of Figures 12.15 and 12.16 illustrates the trade-offs between control action and disturbance attenuation for the designs with cancellation of the fast process pole and active damping. ∇

12.5 DESIGN FOR ROBUST PERFORMANCE

Control design is a rich problem where many factors have to be taken into account. Typical requirements are that load disturbances should be attenuated, the controller should only inject a moderate amount of measurement noise, the output should follow variations in the command signal well and the closed loop system should be insensitive to process variations. For the system in Figure 12.10 these requirements can be captured by specifications on the sensitivity functions S and T and the transfer functions G_{yd}, G_{un}, G_{yr} and G_{ur}. Notice that it is necessary to consider at least six transfer functions, as discussed Section 11.1. The requirements are mutually conflicting and it is necessary to make tradeoffs. Attenuation of load disturbances will be improved if the bandwidth is increased but so will the noise injection.

It is highly desirable to have design methods that can guarantee robust performance. Such design methods did not appear until the late 1980s. Many of these design methods result in controllers having the same structure as the controller based on state feedback and an observer. In this section we provide a brief review of some of the techniques as a preview for those interested in more specialized study.

Linear Quadratic Control (LQG)

One way to make the trade-off between attenuation of load disturbances and injection of measurement noise is to design a controller that minimizes the loss function

$$J = \frac{1}{T}\int_0^T \left(y^2(t) + \rho u^2(t)\right) dt,$$

where ρ is a weighting parameter as discussed in Section 6.3. This loss function gives a compromise between load disturbance attenuation and disturbance injection because it balances control actions against deviations in the output. If all state variables are measured, the controller is a state feedback

$$u = -Kx$$

The controller has the same form as the controller obtained by eigenvalue assignment (pole placement) in Section 6.2. However, the controller gain is obtained by solving an optimization problem. It has been shown that this controller is very robust. It has a phase margin of at least 60° and an infinite gain margin. The controller is called a *linear quadratic control* or *LQ control* because the process model is linear and the criterion is quadratic.

When all state variables are not measured, the state can be reconstructed using an observer, as discussed in Section 7.3. It is also possible to introduce process disturbances and measurement noise explicitly in the model and to reconstruct the states using a Kalman filter as discussed briefly in Section 7.4. The Kalman filter has the same structure as the observer designed by pole assignment in Section 7.3, but the observer gains L are now obtained by solving an optimization problem. The control law obtained by combining linear quadratic control with a Kalman filter is called *linear quadratic Gaussian control* or *LQG Control*. The Kalman filter is optimal when the models for load disturbances and measurement noise are Gaussian.

It is interesting that the solution to the optimization problem leads to a controller having the structure of a state feedback and an observer. The state feedback gains depend on the parameter ρ and the filter gains depend on the parameters in the model that characterize process noise and measurement noise (see Section 7.4). There are efficient programs to compute these feedback and observer gains.

The nice robustness properties of state feedback are unfortunately lost when the observer is added. It is possible to choose parameters that give closed loop systems with poor robustness, similar to Example 12.8. We can thus conclude that there

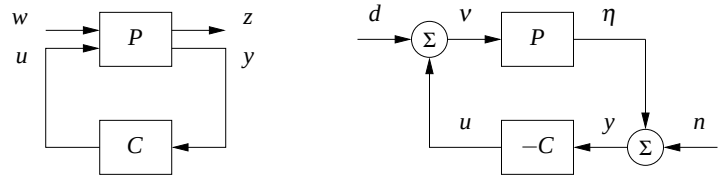

Figure 12.17: H_∞ robust control formulation. The left figure shows a general representation of a control problem used in robust control. The input u represents the control signal, the input w represents the external influences on the system, the output z is the generalized error and the output y is the measured signal. The right figure shows the special case of the basic feedback loop in Figure 12.10 where the reference signal is zero. In this case we have $w = (-n, d)$ and $z = (x, v)$.

is a fundamental difference between using sensors for all states and reconstructing the states using an observer.

H_∞ Control

Robust control design is often called H_∞ control for reasons that will be explained shortly. The basic ideas are simple but the details are complicated and we will therefore just give the flavor of the results. A key idea is illustrated in Figure 12.17 where the closed loop system is represented by two blocks, the process P and the controller C as discussed in Section 11.1. The process P has two inputs, the control signal u which can be manipulated by the controller, and the generalized disturbance w, which represents all external influences, for example command signals and disturbances. The process has two outputs, the generalized error z which is a vector of error signals representing the deviation of signals from their desired values and the measured signal y which can be used by the controller to compute u. For a linear system and a linear controller the closed loop system can be represented by the linear system

$$z = H(P(s), C(s))w \tag{12.21}$$

which tells how the generalized error w depends on the generalized disturbances w. The control design problem is to find a controller C such that the gain of the transfer function H is small even when the process has uncertainties. There are many different ways to specify uncertainty and gain, giving rise to different designs. The names H_2 and H_∞ control correspond to the norms $\|H\|_2$ and $\|H\|_\infty$.

To illustrate the ideas we will consider a regulation problem for a system where the reference signal is assumed to be zero and the external signals are the load disturbance d and the measurement noise n, as shown in Figure 12.17b. The generalized input is $w = (-n, d)$. (The negative sign of n is not essential, but is chosen to get somewhat nicer equations.) The generalized error is chosen as $z = (\eta, v)$, where η is the process output, and v is the part of the load disturbance that is not

compensated by the controller. The closed loop system is thus modeled by

$$z = \begin{pmatrix} \eta \\ \nu \end{pmatrix} = H(P,C) \begin{pmatrix} -n \\ d \end{pmatrix} = \begin{pmatrix} \frac{1}{1+PC} & \frac{P}{1+PC} \\ \frac{C}{1+PC} & \frac{PC}{1+PC} \end{pmatrix} \begin{pmatrix} -n \\ d \end{pmatrix}, \qquad (12.22)$$

which is the same as equation (12.21). A straightforward calculation shows that

$$\|H(P,C))\|_\infty = \sup_\omega \frac{\sqrt{(1+|P(i\omega)|^2)(1+|C(i\omega)|^2)}}{|1+P(i\omega)C(i\omega)|}. \qquad (12.23)$$

There are efficient numerical methods to find a controller such that $\|H(P,C)\|_\infty < \gamma$, if such a controller exists. The best controller can then be found by iterating on γ. The calculations can be made by solving *algebraic Riccati* equations, for example by using the command `hinfsyn` in MATLAB. The controller has the same order as the process and the same structure as the controller based on state feedback and an observer; see Figure 7.7 and equation (7.18) on page 214.

Notice that if we minimize $\|H(P,C)\|_\infty$ we make sure that the transfer functions $G_{yd} = P/(1+PC)$, representing transmission of load disturbances to the output, and $G_{un} = -C/(1+PC)$, representing how measurement noise is transmitted to the control signal, are small. Since the sensitivity and the complementary sensitivity functions are also elements of $H(P,C)$ we have also guaranteed that the sensitivities are also less than γ. The design methods thus balance performance and robustness.

There are strong robustness results associated with the H_∞ controller. We can understand this intuitively by comparing equations (12.1) and (12.23). We can then conclude that

$$\|H(P,C)\|_\infty = \frac{1}{d_\nu(P,-1/C)}. \qquad (12.24)$$

The inverse of $\|H(P,C)\|_\infty$ is thus equal to chordal distance between P and $1/C$. If we find a controller C with $\|H(P,C)\|_\infty < \gamma$ this controller will then stabilize any process P_* such that $d_\nu(P,P_*) < \gamma$.

Disturbance Weighting

Minimizing the gain $\|H(P,C)\|_\infty$ means that gains of all individual signal transmissions from disturbances to outputs are less that γ for all frequencies of the input signals. The assumption that the disturbances are equally important and that all frequencies are also equally important is not very realistic, recall that load disturbances typically have low frequencies and measurement noise is typically dominated by high frequencies. It is straightforward to modify the problem so that disturbances of different frequencies are given different emphasis, by introducing a weighting filter on the load disturbance as shown in Figure 12.17. For example low frequency load disturbances will be enhanced by choosing W_d as a low pass filter because the actual load disturbance is $W_d\bar{d}$.

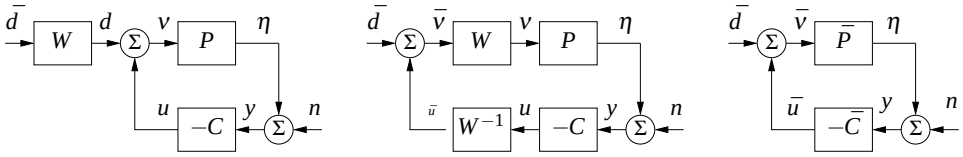

Figure 12.18: Block diagrams of a system with disturbance weighting. The left figure provides a frequency weight on processes disturbances. Through block diagram manipulation, this can be converted to the standard problem on the right.

By using block diagram manipulation as shown in Figure 12.18 we find that the system with frequency weighting is equivalent to the system with no frequency weighting in Figure 12.18 and the signals are related through

$$z_w = \begin{pmatrix} \eta \\ \bar{v} \end{pmatrix} \begin{pmatrix} \dfrac{1}{1+P_wC_w} & \dfrac{P_w}{1+P_wC_w} \\ \dfrac{C_w}{1+P+wC_w} & \dfrac{P_wC_w}{1+P_wC_w} \end{pmatrix} \begin{pmatrix} -n \\ \bar{d} \end{pmatrix} = H(P_w, C_w)w_w, \qquad (12.25)$$

where $P_w = PW_d$ and $C_w = W_d^{-1}C$. The problem of finding a controller C_w that minimizes the gain of $H(P_w, C_w)$ is thus equivalent to the problem without disturbance weighting; having obtained C_w, the controller for the original system is then $C = W_dC$. Notice that if we introduce the frequency weighting $W_d = k/s$ we will automatically get a controller with integral action.

Limits of Robust Design

There is a limit to what can be achieved by robust design. In spite of the nice properties of feedback, there are situations where the process variations are so large that it is not possible to find a linear controller that gives a robust system with good performance. It is then necessary to use other types of controllers. In some cases it is possible to measure a variable that is well correlated with the process variations. Controllers for different parameter values can then be designed and the corresponding controller can be chosen based on the measured signal. This type of control design is called *gain scheduling*. The cruise controller is a typical example where the measured signal could be gear position and velocity. Gain scheduling is the common solution for high performance aircraft where scheduling is done based on Mach number and dynamic pressure. When using gain scheduling it is important to make sure that switches between the controllers do not create undesirable transients (often referred to as *bumpless transfer*).

If it is not possible to measure variables related to the parameters, it is possible to use *automatic tuning* and *adaptive control*. In automatic tuning the process dynamics are measured by perturbing the system and a controller is then designed automatically. Automatic tuning requires that parameters remain constant and it has been widely applied for PID control. It is a reasonable guess that in the fu-

ture many controllers will have features for automatic tuning. If parameters are changing it is possible to use adaptive methods where where process dynamics are measured on-line.

12.6 FURTHER READING

The topic of robust control is a large one, with many articles and textbooks devoted to the subject. Robustness was a central issue in classical control as described in Bode's classical book [Bod45]. Robustness was deemphasized in the euphoria of the development of design methods based on optimization. The strong robustness of controllers based on state feedback shown by Anderson and Moore [AM90] contributed to the optimism. The poor robustness of output feedback was pointed out by Rosenbrock [RM71], Horowitz [Hor75] and Doyle [Doy78] and resulted in a renewed interest in robustness. A major step forward was the development of design methods where robustness was explicitly taken into account, such as the seminal work by Zames [Zam81]. Robust control was originally developed using powerful results from the theory of complex variables, which unfortunately gave controllers of high order. A major breakthrough was given by Doyle, Glover, Khargonekar, and Francis [DGKF89], who showed that the solution to the problem could be obtained using Riccati equations and that a controller of low order could be found. This paper led to an extensive treatment of the so-called H_∞ control, including books by Francis [Fra87], McFarlane and Glover [MG90], Doyle, Francis and Tannenbaum [DFT92], Green and Limebeer [GL95], Zhou, Doyle and Glover [ZDG96], Skogestand and Postlethwaite [SP05], and Vinnicombe [Vin01]. A major advantage of the theory is that it combines much of the intuition from servomechanism theory with sound numerical algorithms based on numerical linear algebra and optimization. The results have been extended to nonlinear systems by treating the design problem as a game where the disturbances are generated by an adversary, as described in the book by Basare and Beernhard [BB91].

EXERCISES

12.1 Consider a feedback loop with a process and a controller having transfer functions P and C. Assume that the maximum sensitivity is $M_t = 2$. Show that the phase margin is at least 30° and that the closed loop system will be stable if the gain is changed by 50%.

12.2 Show that a stable additive perturbation ΔP_{add} can create right half plane zeros, but not right half plane poles, and that a stable feedback perturbation ΔP_{fbk} can create right half plane poles but not right half plane zeros. Give constructive examples of each.

12.3 Compute the μ-gap metric between the systems

$$P_1(s) = \frac{k}{s+1} \quad \text{and} \quad P_2(s) = \frac{k}{s-11}$$

for $k = 1, 2$ and 5.

12.4 The distance measure is closely related to closed loop systems with unit feedback. Show how the measure can be modified to apply to an arbitrary feedback.

12.5 Consider the transfer functions in Examples 12.2 and 12.3. Compute the distance measure $d_\nu(P_1, P_2)$ in both cases. Repeat the calculations when the controller is $C = 0.1$.

12.6 Consider the Nyquist curve in Figure 12.12. Explain why part of the curve is approximately a circle. Derive a formula for the center and the radius and compare with the actual Nyquist curve.

12.7 (Ideal delay compensator) Consider a process whose dynamics are a pure time delay with transfer function $P(s) = e^{-s}$. The ideal delay compensator is a controller with the transfer function $C(s) = 1/(1-e^{-s})$. Show that the sensitivity functions are $T(s) = e^{-s}$ and $S(s) = 1 - e^{-s}$ and that the closed loop system will be unstable for arbitrarily small changes in the delay.

12.8 Let P and C be matrices whose entries are complex numbers. Show that the singular values of the matrix

$$H(P,C) = \begin{pmatrix} \dfrac{1}{1+PC} & \dfrac{P}{1+PC} \\ \dfrac{C}{1+PC} & \dfrac{PC}{1+PC} \end{pmatrix}$$

are

$$\sigma_1 = 0 \qquad \sigma_2 = \sup_\omega \frac{\sqrt{(1+|P(i\omega)|^2)(1+|C(i\omega)|^2)}}{|1+P(i\omega)C(i\omega)|}.$$

12.9 Show that

$$\sup_w \frac{|1+P(i\omega)C(i\omega)|}{\sqrt{(1+|P(i\omega)|^2)(1+|C(i\omega)|^2)}} = d(P, -1/C).$$

12.10 (Bode's ideal loop transfer function) When designing electronic amplifiers Bode proposed that the loop transfer function should have the form $L(s) = ks^{-n}$ with $0 < n < 2$. Show that such a loop transfer function has constant stability margin $s_m = \arcsin \pi(1-n/2)$. Plot the Nyquist curve of the system and determine phase and gain margins.

12.11 Consider the system

$$\begin{aligned} \frac{dx}{dt} &= Ax + Bu = \begin{pmatrix} -1 & 0 \\ 1 & 0 \end{pmatrix} x + \begin{pmatrix} a-1 \\ 1 \end{pmatrix} u \\ y &= Cx = \begin{pmatrix} 0 & 1 \end{pmatrix} y. \end{aligned} \tag{12.26}$$

The system has the transfer function

$$G_P(s) = C[sI - A]^{-1}B = \frac{s+a}{s(s+1)} \tag{12.27}$$

12.12 Rewrite the solution below as an exercise.

12.13 (Disk drive tracking) Insert from CDS 110a, using sensitivity. Noise $\rightarrow$ sensitivity spec $\rightarrow$ design $\rightarrow$ robustness check.